HADRON PRODUCTION IN DEEP INELASTIC SCATTERING OF 150 GeV MUONS IN NUCLEAR EMULSION*

By L. Hand, D. Petersen, H. Scott, E. Friedlander**

Laboratory of Nuclear Studies, Cornell University, Ithaca, New York 14853, USA

M. Atac, A. L. Read, L. Voyvodic

Fermi National Accelerator Laboratory, P. O. Box 500, Batavia, Illinois 60510, USA

W. Czyż, B. Furmańska, R. Hołyński, A. Jurak, S. Krzywdziński, G. Nowak, H. Wilczyński, W. Wolter, B. Wosiek

Institute of Nuclear Physics, Cracow***

R. Ball, J. Kiley, A. Kotlewski, L. Litt

Physics Department, Michigan State University, East Lansing, Michigan 48823, USA

J. Florian, J. J. Lord, R. J. Wilkes

Physics Department FM-15, University of Washington, Seattle, Washington 98195, USA

(Received August 29, 1978)

Multiparticle production from an experiment designed to search for charmed particles is described and analyzed. A nuclear emulsion stack was bombarded with the Fermilab 150 GeV μ^+ beam and a system of counters, proportional chambers and drift chambers, and a magnetic spectrometer were used to detect and momentum analyze the scattered muons. Multiplicity distributions are given and compared with results of proton- and π^--emulsion interactions at equivalent energies. A comparison of the pseudo-rapidity distributions is also made. Although there is an over-all similarity between muon and hadron induced multiparticle production on nuclei there are also some clearly marked differences: e. g., muons are, on the average, less efficient than hadrons in producing particles on nuclei. Knowing the angles and energies of the scattered muons we are able to select the processes in which particle multiplication must occur through intra-nuclear cascading. Our data indicate that cascading does exist as one of the effective mechanisms of particle multiplication in μ-nucleus collisions. Further experiments investigating the mechanism of this cascading are of considerable interest.

* Work supported in part by the Polish-American M. Skłodowska-Curie Fund, NSF Grant No OIP75-01319.

** Now at Lawrence, Berkeley Laboratory, University of California, Berkeley, USA.

*** Address: Instytut Fizyki Jądrowej, Kawiory 26A, 30-055 Kraków, Poland.

1. Introduction

While multihadron production processes generated on nuclear targets by incident high energy hadrons have a long history (see e.g. Ref. [1]) the lepton data on multihadron production from high energy lepton-nucleus interactions are rather scarce. It seems therefore interesting to present all the available characteristics of multihadron production in deep inelastic scattering of muons in nuclear emulsion and compare them with the data for hadron-emulsion interactions. This is the main topic of this paper.

The muon data reported here were obtained as a byproduct from a hybrid electronic--emulsion experiment designed to search for charmed particles [2] and performed at Fermilab with 150 GeV μ^+ beam. The availability of high energy muon beams at Fermilab has permitted an extension of studies of muonic interactions to higher ν, W^2 and Q^2 values than are accesible at electron machines. We use the standard notation, where

$$s = W^2 = 2m\nu + m^2 - Q^2 \tag{1}$$

is the invariant mass squared of the hadronic final state,

$$Q^2 = 2EE'(1-\cos\theta_\mu) \tag{2}$$

is the four momentum transfer squared,

$$\nu = E - E' \tag{3}$$

is the energy loss of the muon, and m is the nucleon mass.

Interactions of various high energy projectiles with nuclei provide us with important information on space-time evolution of the hadron final states [3–6]. When the incident particle is a hadron the main bulk of production on nuclear targets comes presumably from a mechanism in which large longitudinal interaction regions of the incident particles are involved [3]. There may, however, exist some other production mechanisms where short interaction regions are relevant, for instance intra-nuclear cascading. By cascading we understand the following mechanism of production: the incident particle interacts with just one nucleon of the target and the products of this interaction, not the incident particle, collide with the other nucleons of the target and produce more particles. The nature of these intermediate products is of great importance for understanding of the space-time development of production processes. However, in hadron induced production, it is rather difficult to identify processes of cascading. On the other hand, in the lepton induced processes where lepton momentum transfers and energy losses are measured, there is a possibility of identifying cascading. This is because to a very good approximation charged leptons interact via exchange of one photon and by varying the mass $-Q^2$ and energy ν of the virtual photon one can analyze multihadron production processes for short or long lived, very massive or almost real virtual photons. We take advantage of these possibilities and, as discussed in Refs [4–6], by selecting muon–nucleus interactions with small enough Bjorken scaling variable $\omega = 2m\nu/Q^2$ we deal with processes in which the virtual photon interacts with only one nucleon of the target nucleus. Thus, although our statistics are low, our analysis nevertheless extracts some important effects as, for example, intra-nuclear cascading, which deserve a more thorough investigation.

The paper is organized as follows. In Section 2 we give the notation we use for the multiplicities. In Section 3 we describe briefly the experimental setup. In Section 4 the results on multiplicity distributions are collected and compared with the analogous data for incident hadrons. In Section 5 the pseudo-rapidity distributions are given and compared with the results of multiparticle production by hadrons in emulsion and by muons on hydrogen. Section 6 contains discussion and conclusions.

2. *Notation*

Throughout the paper we shall use the following notation for the multiplicities and the following relations between them:

n_s – number of relativistic (minimum ionizing, $\beta \gtrsim 0.7$) particles observed in interactions with emulsion,

N_h – number of slow (heavy ionizing) particles ($\beta < 0.7$); majority of them are fragments of the struck nucleus,

n – number of relativistic charged hadrons. For hadron induced interactions $n = n_s$; for muon induced interactions $n = n_s - 1$ (the scattered muon is subtracted from n_s),

n_{ch} – multiplicity of charged hadrons, in hadron-hydrogen and muon-hydrogen interactions,

$\langle n_s \rangle - 1$ – average multiplicity of produced charged hadrons in both muon-emulsion and hadron-emulsion interactions. Since most of the recoil protons are slow and do not contribute to n_s only the incident surviving particle is subtracted from n_s. One should realize, however, that in the interactions with small ω a considerable fraction of the recoiling protons may be relativistic and included in n_s [7]. Although this correction is difficult to compute we can accept that, by taking all recoiling protons as relativistic, one underestimates the number of produced hadrons. So, for small ω's, we shall take $\langle n_s \rangle - 1.5$, instead of $\langle n_s \rangle - 1$, for the number of produced hadrons in μ — nucleus interactions. This correction is valid for a target with equal number of protons and neutrons. For hadron-nucleus interactions one can neglect this effect because there one never deals with samples which are rich in relativistic recoiling protons,

$\langle n_{ch} \rangle - 0.5$ – average multiplicity of produced charged particles in muon-proton and muon-neutron interactions. Note that in accordance with Ref. [8] we remove the recoiling proton by subtracting 0.5 (not 1) from $\langle n_{ch} \rangle$. This is because the exchange interactions are important for 2.5 GeV $\lesssim W \lesssim$ 4.25 GeV and we assume this to hold also for larger W. To compute the relative multiplicities, R, which measure the influence of the target nucleus on production, we need to know the average multiplicity on one "effective nucleon". This multiplicity for a target composed of Z protons and $A-Z$ neutrons is $\langle n_{nucl} \rangle = \dfrac{Z\sigma_p \langle n_p \rangle + (A-Z)\sigma_n \langle n_n \rangle}{Z\sigma_p + (A-Z)\sigma_n}$, where subscripts refer to proton or neu-

tron. In the case of muon-emulsion interactions we therefore take $\langle n_{nucl} \rangle \cong \langle n_{ch} \rangle - 0.5$,

$\langle n_{ch} \rangle - 2$ – average multiplicity of produced charged hadrons in hadron-proton and hadron-neutron interactions equal to the average multiplicity of charged hadrons in hadron-"effective nucleon" collisions in emulsion.

3. *Description of the experiment*

A hybrid electronic-emulsion experiment was performed with the Fermilab 150 GeV μ^+ beam, in which a system of counters, proportional and drift chambers and a magnetic spectrometer were used to detect and momentum analyze muons scattered in nuclear emulsion targets. A total of 5.6 liters of emulsion, divided into 26 emulsion stacks, was exposed, yielding a sample of 91 deep inelastic events. Each stack was composed of 80–100 Ilford K5 pellicles of dimensions $7.5 \times 5 \times 0.06$ cm^3 (5 cm in the beam direction).

The experimental arrangement is shown in Fig. 1. The trigger used was $C \cdot S \cdot BV \cdot HV$, $C = C_1 \cdot C_2 \cdot C_3 \cdot C_4 \cdot C_5$, $BV = BV_1 \cdot BV_2$, $S = SA \cdot SB \cdot SC$, etc.; i. e., a single in-

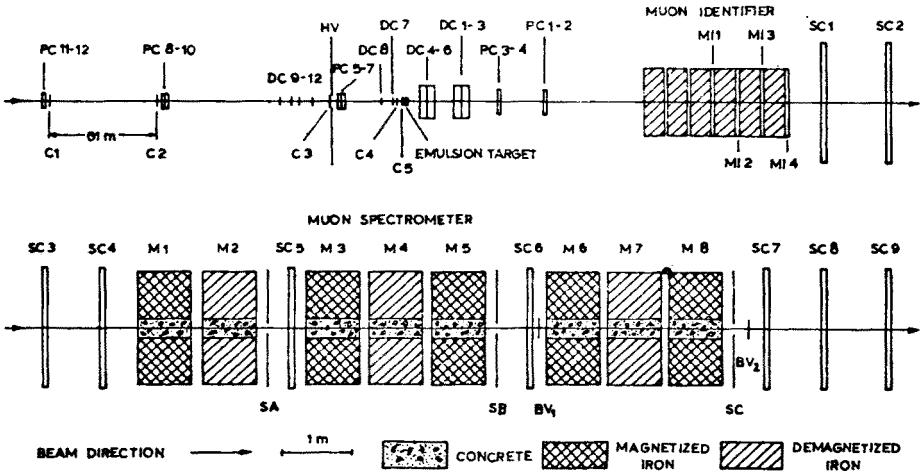

Fig. 1. Experimental arrangement of FNAL experiment 382. PC1–PC12 — proportional chambers, DC1–DC12 — drift chambers, SC1–SC9 — spark chambers, C1–C5 — beam counters, HV — halo veto counter, BV1, BV2 — beam veto counters, MI1–MI4 — muon identifier counters, M1–M8 — spectrometer magnets

-geometry incoming track, and scattered muon detected in the magnetic spectrometer unaccompanied by undeflected penetrating particles. The moun beam had a hadron contamination of less than one part in 10^{-6}.

Triggers were selected as candidates for emulsion scanning according to the following criteria: 1) projected angles of the beam track within 3 mrad of the surveyed beam direction, 2) scattered muon momentum greater than 10 GeV, 3) no tracks within 3 mm

of the projected beam track location in the downstream drift chambers. Event vertexes were found by area scanning along the beam track trajectory defined by the upstream proportional and drift chambers. For each event search, a minimum emulsion volume of 90 mm^3 (1 mm × 50 mm on each of 3 adjacent plates) was scanned, with the volume increased if no candidates were found on the first pass. Scanning was performed under 225-fold magnification. When an event candidate was found, tagging was verified by comparing the angle of the scattered muon measured by the muon spectrometer with the track angles seen in the emulsion plate. From a list of 262 scanning candidates, 91 interaction vertexes were found. Details of the apparatus and event locating technique are given elsewhere [2].

The muon spectrometer had momentum resolution $\Delta p/p = 15\%$, whereas angles θ_μ of scattered mouns were measured with an accuracy of about 2 mrad. That implies the following typical uncertainties of variables characterizing an event: $\Delta Q^2/Q^2 \approx 30\%$, $\Delta W/W \approx 60\%$ at $W < 10$ GeV and improving to $\approx 6\%$ at $W > 10$ GeV, $\Delta\omega/\omega \approx 150\%$ at small ω's ($\omega < 10$) and falling to $\approx 40\%$ at $\omega > 50$. In calculating averages of different parameters and their errors individual event uncertainties were taken into account.

4. *Multiplicities*

For each tagged event the number of heavy ionizing tracks N_h was recorded and angles of minimum ionizing tracks n_s were measured and calculated relatively to the direction of the virtual photon.

Fig. 2 shows the integral distribution of N_h. Due to the area scanning technique used to locate events, biases against events with low N_h are expected. One of the fundamental

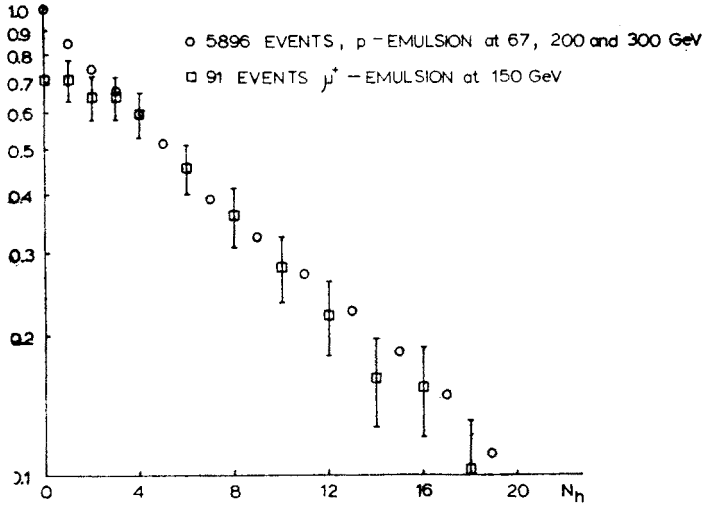

Fig. 2. Integral N_h distribution, $P(\geqslant N_h)$. Proton data comes from a pooled unbiased sample of 5896 proton interactions at 67, 200 and 300 GeV, Refs [13–15,24]. Muon data (91 events) is normalized to give $P_\mu(\geqslant 4) = P_p(\geqslant 4)$

results from emulsion studies of hadronic interactions is the invariance of the N_h distribution over a wide energy range [9–12]. In Fig. 2 a comparison is made with the N_h distribution obtained from a pooled unbiased sample of about 6000 proton-emulsion interactions at 67, 200 and 300 GeV, found in along-track scanning [13–15]. Both distributions have, within the errors, the same slope for $N_h \geqslant 3$. The apparent deviation of the N_h distribution for muon induced interactions with N_h less than about 3 reflects scanning bias, therefore all other data presented here is based on the sample of 88 events with $N_h \geqslant 3$.

Fig. 3 shows the distribution of Q^2 and W for the final sample of 88 events. The kinematical range covered in this experiment is the following: $0.6 < Q^2 \lesssim 21$ GeV^2, $2.5 < W \lesssim 16$ GeV. The mean value of W for our data is $\langle W \rangle = 10.2$ GeV. Since the energy available for hadron production is approximately equivalent to that in 60 GeV

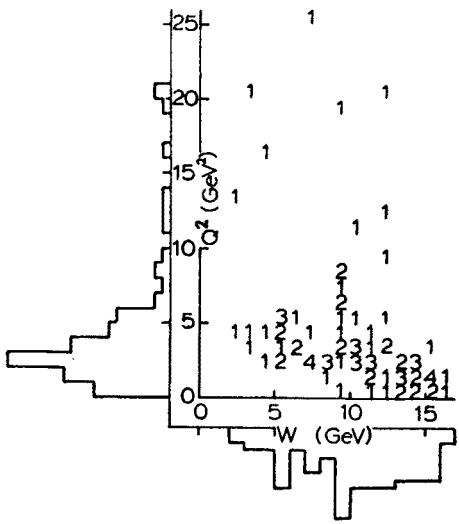

Fig. 3. Scatter plot of Q^2 versus W for 88 muon-emulsion events with $N_h \geq 3$

pion-emulsion interactions ($\sqrt{s} = 10.7$ GeV) and 67 GeV proton-emulsion interactions ($\sqrt{s} = 11.3$ GeV), we use these two sets of data in making various comparisons throughout this paper [12–14].

For multiparticle production on nuclei by incident hadrons many authors have shown that the number of produced particles is correlated with N_h which is a measure of the nuclear excitation of the target nucleus [9, 10, 13, 16, 17]. In Fig. 4 we show the $\langle n \rangle$ vs N_h-dependence for muon, pion and proton induced interactions. All three sets of data show a linear correlation, but the N_h dependence of muon interactions is clearly weaker than in hadron interactions. In Table I, the multiplicity distribution parameters $\langle N_h \rangle$, $\langle n \rangle$, $D = \langle n^2 \rangle - \langle n \rangle^2$ and $f_2 = \langle n(n-1) \rangle - \langle n \rangle^2$ are shown for this experiment, and for the equivalent-energy hadron interactions. Table I also gives the average normalized multiplicities $\langle R \rangle$ calculated for produced hadrons in μ-emulsion, π^--emulsion and p-emul-

sion interactions. R measures the influence of the target nucleus on multiplicity and is defined as follows:

$$R_{\mu(h)} = \frac{\text{multiplicity of produced hadrons in } \mu \text{ (hadron)-emulsion interaction}}{\text{average multiplicity of produced hadrons in } \mu \text{ (hadron)-"effective nucleon" interactions}}$$

Thus for muon and hadron interactions we have:

$$\langle R_\mu \rangle = \left\langle \frac{n_s - 1}{\langle n_{\text{nucl}} \rangle} \right\rangle = \left\langle \frac{n_s - 1}{\langle n_{\text{ch}} \rangle - 0.5} \right\rangle, \quad \langle R_h \rangle = \frac{\langle n_s \rangle - 1}{\langle n_{\text{nucl}} \rangle} = \frac{\langle n_s \rangle - 1}{\langle n_{\text{ch}} \rangle - 2}. \tag{4}$$

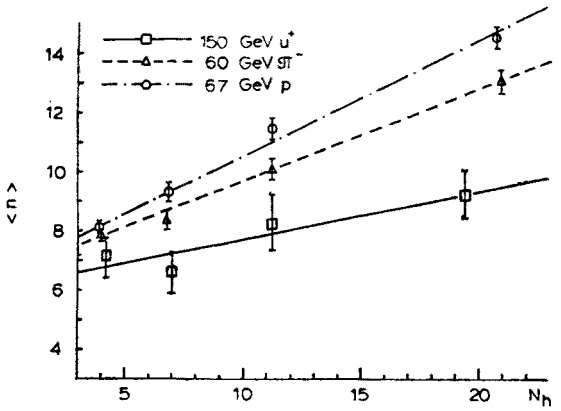

Fig. 4. $\langle n \rangle$ versus N_h dependence for muon induced reactions compared with 60 GeV π^- and 67 GeV p data, Refs [12–14]. All data are for $N_h \geqslant 3$

Since data on multiparticle production by electrons and muons on proton targets is not available at all energies we need, we used $\langle n_{\text{ch}} \rangle$ calculated from the formula similar to the "universal" fit of Ref. [18]:

$$\langle n_{\text{ch}} \rangle = 2.3 + 0.28 \ln E_{\text{ab}} + 0.53 \ln^2 E_{\text{ab}}, \tag{5}$$

where $E_{\text{ab}} = \sqrt{s} - m_a - m_b$ is the CM energy available for particle production and m_a, m_b are the masses of the initial state particles ($E_{\text{ab}} = W - m$ for muon-proton interactions). Eq. (5) gives a good representation of the average charged hadron multiplicity in muon-proton interactions in the energy range of W from 2.5 GeV up to 4.25 GeV [8, 19]. The only difference with Ref. [18] is the constant term which we adjusted to fit the data of Ref. [8, 19]. We also use (5) for still higher energies where there are no data for muon-proton interactions, and assume that $\langle n_{\text{ch}} \rangle$, for a given W, does not depend on Q^2 [1].

[1] For electron-hydrogen and muon-hydrogen interactions this is well established for $Q^2 \lesssim 8$ GeV^2 [8, 19, 20]. We accept here the independence of $\langle n_{\text{ch}} \rangle$ on Q^2 for all values of Q^2 of our experiment. One should also stress that in neutrino-hydrogen interactions [21] the independence of $\langle n_{\text{ch}} \rangle$ on Q^2 is established up to about 35 GeV^2, completely covering the range relevant in our experiment.

TABLE I

Multiplicity parameters for muon and equivalent energy hadron interactions in emulsion. All data are for $N_h \geqslant 3$

	No. of events	$\sqrt{s}$, W GeV	$\langle N_h \rangle$	$\langle n \rangle$	D	f_2	$\langle R \rangle$	$\langle Q^2 \rangle$ GeV^2	$\langle \omega \rangle$
μ-Em	88	11.1 ±0.4	10.2 ±0.7	7.8 ±0.5	4.2 ±0.3	9.2 ±2.7	1.59 ±0.12	3.9 ±0.5	55 ±12
μ-Em $9 \leqslant W \leqslant 14$	43	11.5 ±0.3	9.8 ±1.1	7.9 ±0.7	4.3 ±0.6	9.8 ±4.6	1.55 ±0.13	4.3 ±0.7	54 ±11
π^--Em 60 GeV	544	10.7	10.3 ±0.3	9.6 ±0.2	5.2 ±0.2	17.3 ±2.2	2.10 ±0.10	—	—
p-Em 67 GeV	801	11.3	10.7 ±0.3	10.9 ±0.2	5.8 ±0.2	22.9 ±2.0	2.53 ±0.07	—	—

Since muon events have different CM energies W of the hadronic final state, the values R_μ were calculated for each event separately and then the average $\langle R_\mu \rangle$ taken. Thus unlike the $\langle R_h \rangle$ of multiparticle production by hadrons, which is monoenergetic, $\langle R_\mu \rangle$ represents an average over energy as well as multiplicity. The values of $\langle R \rangle$, given in Table I for both muon and hadron interactions, are larger than unity which means that in all cases we have multiplications of particles, but the multiplication is weaker in muon induced interactions.

In order to get more information about the physical nature of the particle multiplication process we grouped the muon interactions according to the Bjorken scaling variable

TABLE II

Relative hadron multiplicity $\langle R \rangle$ in muon-emulsion interactions with $N_h \geqslant 3$ for five ω intervals

ω interval	No. of events	$\langle \omega \rangle$	$\langle W \rangle$ GeV	$\langle Q^2 \rangle$ GeV^2	$\langle N_h \rangle$	$\langle n \rangle$	$\langle R \rangle$
$\omega < 10$	18	4.3 ±1.3	7.0 ±1.0	8.8 ±1.8	10.1 ±1.1	7.3 ±0.8	1.92 ±0.41
$10 \leqslant \omega < 25$	20	14.5 ±2.1	9.4 ±0.6	5.3 ±0.7	9.7 ±1.7	7.0 ±0.8	1.56 ±0.20
$25 \leqslant \omega < 50$	17	34.1 ±4.1	10.8 ±0.4	3.2 ±0.3	10.5 ±1.6	7.0 ±0.9	1.43 ±0.20
$50 \leqslant \omega < 150$	17	82 ±10	12.9 ±0.5	1.9 ±0.2	11.2 ±1.9	9.1 ±1.3	1.68 ±0.24
$\omega > 150$	16	227 ±42	14.6 ±0.3	0.9 ±0.1	9.4 ±1.3	8.9 ±1.0	1.52 ±0.17

ω. As discussed in Ref. [6] this variable is related to the lifetime τ of the virtual photon by $\omega \approx m\tau$. Thus ω determines a distance over which the virtual photon can interact coherently. In fermis this distance is $r = \omega/5$. When $\omega \lesssim 5$ the virtual photon interacts with just one nucleon. In Table II the average multiplicity $\langle n \rangle$ and $\langle R \rangle$'s, for 5 bins of ω as well as some other relevant parameters are given. The average multiplicities $\langle n \rangle$ vs $\langle \omega \rangle$ presented in Table II are also shown in Fig. 5 together with dependence of $\langle n_{\text{nucl}} \rangle = \langle n_{\text{ch}} \rangle - 0.5$ on ω calculated from Eq. (5) using mean values of W in a given

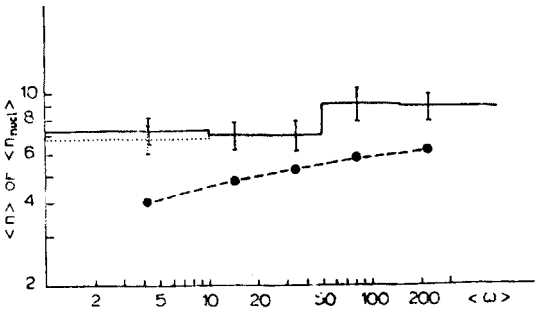

Fig. 5. Mean multiplicities of produced hadrons $\langle n \rangle$ in muon-emulsion interactions (solid line) plotted versus $\langle \omega \rangle$, together with mean multiplicities $\langle n_{\text{nucl}} \rangle$ of produced hadrons in muon-nucleon interactions (dots connected by a dashed line) calculated from (5) for the value of $\langle W \rangle$ in a given ω bin. The two values for $\langle n \rangle$ at the lowest ω bin (solid and dotted lines) show the estimates of the upper and the lower bounds of $\langle n \rangle$

ω-bin. One can see from Table II (cf. values of $\langle R \rangle$) and Fig. 5 that the multiplication of particles takes place ($\langle n \rangle > \langle n_{\text{nucl}} \rangle$) in every ω-bin. The interpretation of the mechanism of multiplication at small ω will be discussed in Section 6 (see also Ref. [22]).

5. *Angular dependences and distributions*

In emulsion experiments, where only the angles of individual tracks are measured, the pseudo-rapidity variable

$$\eta = -\ln \tan \frac{\theta_{\text{lab}}}{2} \tag{6}$$

is a useful approximation to the true rapidity

$$y = \tfrac{1}{2} \ln \frac{E + p_{\parallel}}{E - p_{\parallel}} \tag{7}$$

for tracks with $m^2/p_{\perp}^2 \ll 1$. For muon events θ_{lab} is calculated relative to the virtual photon direction, as determined from the muon scattering angle and momentum.

Fig. 6 shows the pseudo-rapidity distribution $\frac{1}{N} \frac{dn}{d\eta}$ of the relativistic hadrons (scat-

tered muons are excluded) for all events with $N_h \geqslant 3$, compared with equivalent-energy pion and proton data. N is the number of events, hence the distribution is normalized to one event.

The muon- and hadron-induced distributions coincide in the extreme forward direction. In the backward direction the muon and pion data are also compatible, while the proton data appear to be somewhat higher. The majority of additional tracks in hadron interactions (reflecting the higher $\langle n \rangle$) appears in the central and near-forward regions.

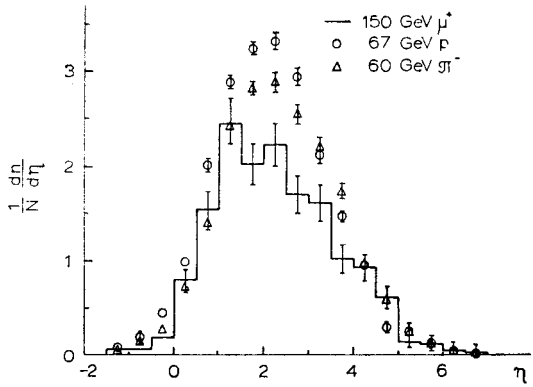

Fig. 6. η distribution for muon-emulsion events with $N_h \geqslant 3$ compared with 60 GeV π^- and 67 GeV p data, Refs [12–14]

The muon data shown in Fig. 6 covers a broad range of W, and a completely satisfactory estimate of the distortions introduced by such averaging cannot be made, because there is insuffcient data on hadron-emulsion interactions in the appropriate energy range to construct an equivalently averaged sample. Nor do adequately reliable models exist to compute corrections. Nevertheless, our data show that these distortions are relatively unimportant; in Fig. 7 we compare a sample of 43 muon events with $9 < W < 14$ GeV,

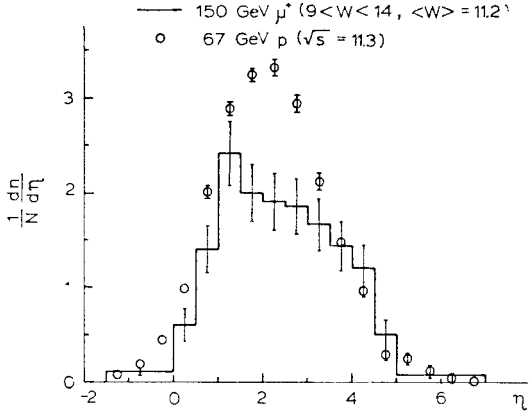

Fig. 7. η distribution for 43 muon-emulsion events with $9 < W < 14$ GeV, $\langle W \rangle = 11.2$ compared with 67 GeV proton-emulsion data, $W = 11.3$, Refs [13, 14]

$\langle W \rangle$ = 11.2 GeV, with the p-emulsion data at 67 GeV ($\sqrt{s}$ = 11.3). Within errors, the situation seen in Fig. 6 also holds for this equivalent energy comparison. Thus the differences between muon-emulsion and hadron-emulsion rapidity distributions and multiplicity parameters shown in Fig. 6 and Table I are not introduced by the fact that the muon data cover a broad energy range. On the other hand, it is important to note that hadron multiplicities in interactions induced by electrons, muons and hadrons on hydrogen at lower W's show no significant differences when compared at equivalent CM energy of the produced hadronic system [19, 20].

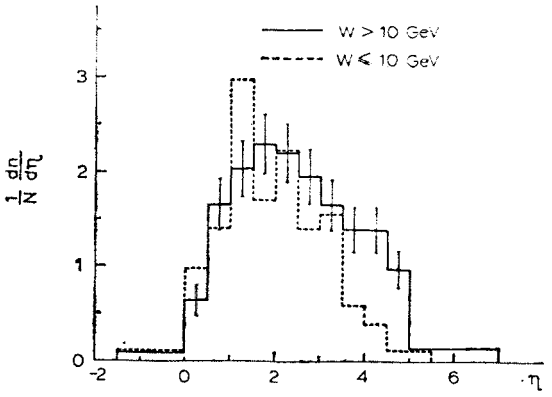

Fig. 8. η distributions for two W bins, $W \leqslant 10$ GeV and $W > 10$ GeV

In order to compare qualitatively the energy dependence of hadron- and muon-induced pseudo-rapidity distributions we have divided our events into two energy bins, $W > 10$ and $W \leqslant 10$ GeV, and plotted their pseudo-rapidity distributions in Fig. 8. The multiplicity parameters for these energy bins are given in Table III. In Fig. 8 one observes that

TABLE III

Multiplicity parameters of muon-emulsion interactions with $N_h \geqslant 3$, for two energy bins

W interval	No. of events	$\langle W \rangle$ GeV	$\langle N_h \rangle$	$\langle n \rangle$	D	f_2	$\langle R \rangle$	$\langle Q_2 \rangle$ GeV^2	$\langle \omega \rangle$
$2 < W < 10$	41	8.0 ±0.5	10.2 ±0.9	6.9 ±0.6	3.8 ±0.3	6.3 ±2.3	1.66 ±0.21	5.4 ±0.9	12.4 ±3.3
$10 \leqslant W < 16.5$	47	13.2 ±0.3	10.2 ±1.0	8.6 ±0.7	4.5 ±0.5	10.4 ±4.1	1.56 ±0.12	2.7 ±0.5	100 ±20

the right-hand side of the distribution shifts with an increase of energy, while the left-hand side remains stationary.

Comparison of μ-emulsion production with μ-hydrogen production at the same incident energy can be made only for the region of pseudo-rapidities limited to the extreme forward direction. This region was covered in the recent experiment [23] on mul-

tiparticle production in μ-hydrogen interactions at 150 GeV [2]. Fig. 9 shows the same sample of μ-emulsion and hadron-emulsion events as in Fig. 6 and the data from Ref. [23]. The distributions are presented in the $\delta\eta$ (or δy) $= \eta(\text{or } y) - y_{\max}$ variable, where $y_{\max}$ is the maximum possible rapidity for a produced pion. As with hadron-hydrogen and hadron-nucleus interactions, the muon-hydrogen distribution in the forward direction coincides with muon-emulsion distribution.

To study where in the pseudo-rapidity distribution the nuclear effects show up we recall the dependence, well known from hadron-emulsion interactions, of nuclear effects on the number of heavy ionizing tracks N_h. Average multiplicities and angular distributions of

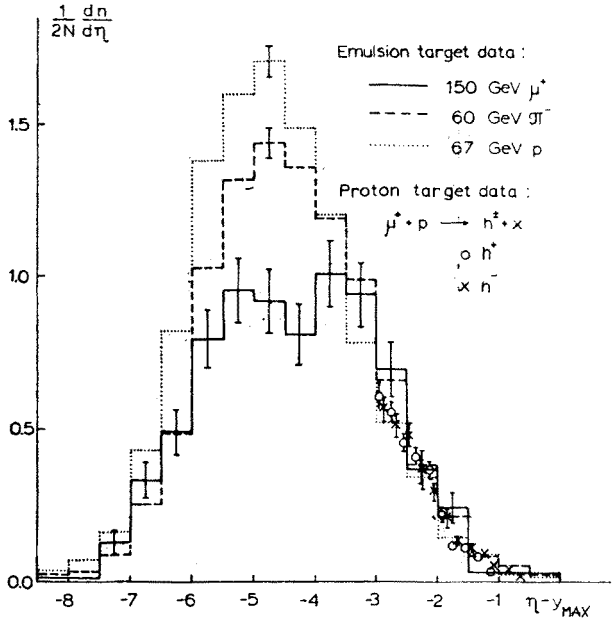

Fig. 9. Distributions of pseudorapidity (rapidity) relative to the maximum possible rapidity. In the forward direction the emulsion data are compared with muon-proton data of Ref. [23]

interactions having small N_h are close to those in hadron-hydrogen reactions, whereas interactions with high N_h (e. g. $\gtrsim 6$) deviate in their characteristics from collisions with hydrogen target. The most pronounced differences which increase with increasing N_h appear in the small rapidity regions [24, 25].

In Figs 10a, b pseudo-rapidity distributions of μ-emulsion interactions with $N_h = 3 \div 8$ and $N_h > 8$ are shown, and in Figs 11 and 12 the ratio:

$$\varrho(\eta) = \frac{\left.\frac{1}{N}\frac{dn}{d\eta}\right|_{N_h > 8}}{\left.\frac{1}{N}\frac{dn}{d\eta}\right|_{N_h = 3 \div 8}}, \tag{8}$$

[2] The data taken for comparison from Ref. [23] cover the following kinematical range: $Q^2 > 0.3$ GeV^2, $W > 10$ GeV, $\omega > 40$.

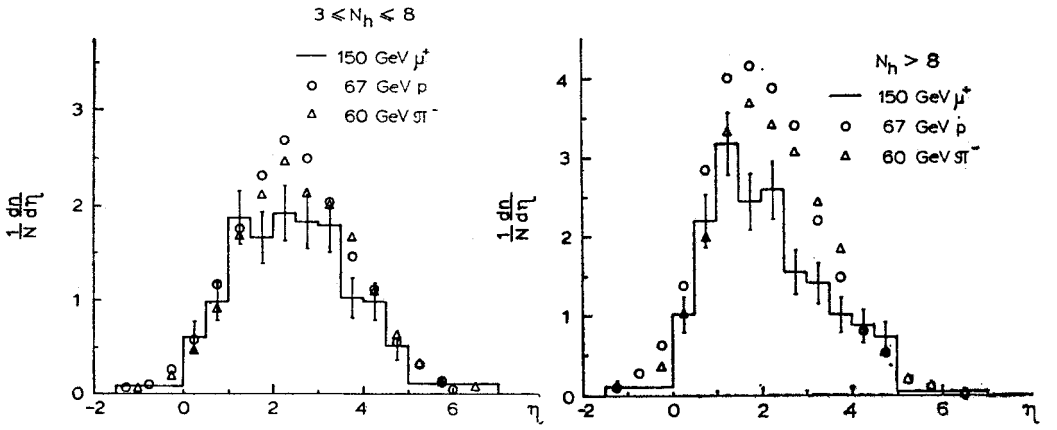

Fig. 10. η distributions for incident muons, protons [13, 14] and pions [12]: (a) events with $3 \leqslant N_h \leqslant 8$; (b) the same for $N_h > 8$

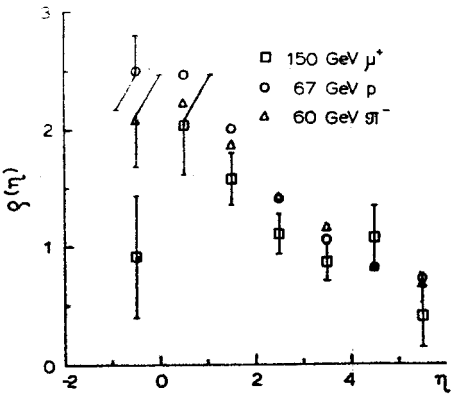

Fig. 11. Ratio ϱ of the distributions show in Figs 10a, b as a function of η. See text for the definition of ϱ.

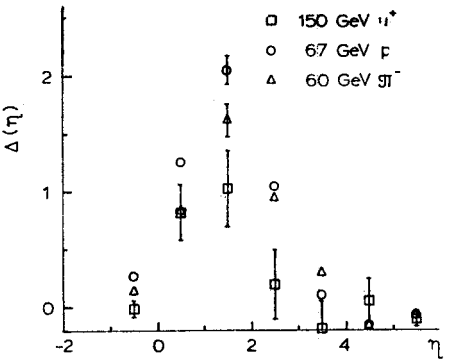

Fig. 12. Difference Δ between the distributions shown in Figs 10a, b as a function of η. See text for the definition of Δ

and the difference:

$$\Delta(\eta) = \frac{1}{N}\frac{dn}{d\eta}\bigg|_{N_h>8} - \frac{1}{N}\frac{dn}{d\eta}\bigg|_{N_h=3\div5} \tag{9}$$

are plotted and compared with hadron induced reactions. Both $\varrho(\eta)$ and $\Delta(\eta)$ reveal similar behaviour for different projectiles. The increase of multiplicity due to nuclear effects is localized in the range of small values of η (below 2.5). These effects are smaller in muon induced interactions, but nevertheless significant and clearly seen.

Another way of looking for nuclear effects, without being limited to the small angle region covered by μ-hydrogen data [23], is to study the $\langle n\rangle$ vs N_h correlation in different

TABLE IV

Results of fits to $\langle n\rangle = a+bN_h$

Data	a	b	χ^2/DF
μ–Em			
$N_h \geqslant 3$, all W	6.10±0.73	0.16±0.07	0.6
π^-–Em			
60 GeV, $N_h \geqslant 3$	6.51±0.25	0.31±0.03	0.5
p–Em			
67 GeV, $N_h \geqslant 3$	6.65±0.24	0.39±0.02	0.9
$\eta < 1.2$			
μ–Em	0.55±0.27	0.12±0.03	0.1
π^-–Em	0.58±0.12	0.12±0.01	0.7
p–Em	0.55±0.12	0.17±0.01	1.8
$1.2 \leqslant \eta < 2.1$			
μ–Em	1.21±0.33	0.08±0.03	0.3
π^-–Em	1.25±0.14	0.12±0.02	0.3
p–Em	1.34±0.13	0.15±0.01	0.9
$2.1 \leqslant \eta < 3.2$			
μ–Em	2.45±0.40	−0.05±0.03	0.4
π^-–Em	2.08±0.13	0.09±0.01	0.0
p–Em	2.33±0.13	0.09±0.01	1.6
$3.2 \leqslant \eta$			
μ–Em	1.95±0.44	−0.01±0.04	0.5
π^-–Em	2.61±0.10	−0.01±0.01	0.0
p–Em	2.36±0.10	−0.01±0.01	4.4

η intervals. In Fig. 13 $\langle n \rangle$ vs N_h dependence in four η bins is presented, together with data for pion and proton projectiles. For $\eta < 2.1$ (backward hemisphere in the CM) $\langle n \rangle$ depends linearly on N_h for both muon and hadron produced events. On the other hand,

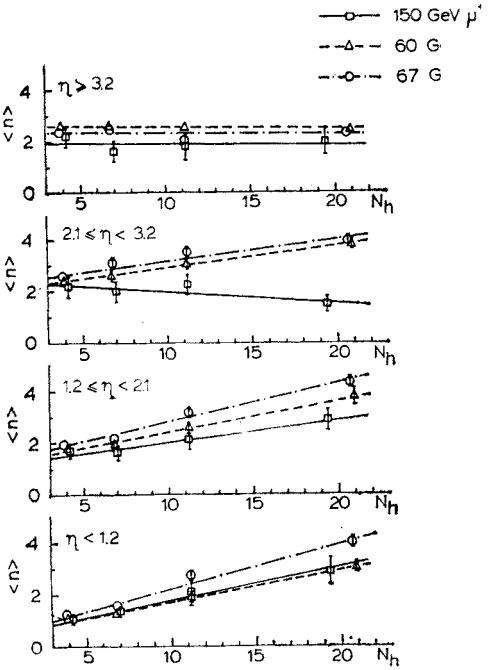

Fig. 13. $\langle n \rangle$ versus N_h for four η bins compared with 60 GeV π^- and 67 GeV p data, Refs [12–14]

the muon data becomes N_h independent above $\eta \approx 2.1$, while the hadron data remain N_h dependent up to $\eta \approx 3.2$. Table IV gives the parameters of the fitted curves. Once again a qualitative similarity between multiparticle production by leptons and hadrons on nuclei is seen.

6. Discussion and conclusions

There is an over-all similarity between muon- and hadron-induced multiparticle production on nuclei, but there are also some clearly marked differences.

First let us discuss the similarities. There are two: The first is that the distributions of N_h for incident hadrons over a wide energy range and for the muons of this experiment are compatible (see Fig. 2). The observed deviations for N_h less than about 3 are due to biases introduced by area scanning. The second is the coincidence of the pseudo-rapidity distributions for the extreme forward directions for hydrogen and nuclear targets (see Fig. 9). Within experimental errors these distributions whether muon- or hadron-induced, coincide. There is also similarity between the energy dependence of muon- and hadron-induced pseudo-rapidity distributions: the right-hand side of the distribution shifts with an increase of energy to the right, while the left-hand side remains stationary [24, 25] (see Fig. 8). There is not enough data for a quantitative comparison.

Then, there are many features of muon-and hadron-induced production which, though qualitatively similar, are quantitatively different: all $\langle R \rangle$'s are larger than unity which means that in all cases we have multiplication of particles in nuclei but all $\langle R \rangle$'s are significantly different from each other and can be ordered as follows:

$$\langle R_\mu \rangle < \langle R_\pi \rangle < \langle R_p \rangle. \tag{10}$$

The pseudo-rapidity distributions for all three projectiles coincide in the extreme forward direction and are compatible in the backward direction, but in the central and near-forward regions there are significant differences (see Fig. 6). Also, there is a qualitative similarity of the correlation of $\langle n \rangle$ with N_h, but quantitatively these correlations are weaker in muon-induced production.

Now let us discuss those results which cannot be directly compared with any hadron--induced production; these are contained in Table II and Fig. 5. As we have already pointed out, by evaluating $\langle R \rangle$'s for various bins of ω we ordered them according to the distances over which the virtual photon can interact coherently. The lowest ω bin corresponds therefore to interactions of the muon with just one nucleon, because the distance $\langle r \rangle = 1$ fm. As one can see from Fig. 5 $\langle n \rangle$ is always larger than $\langle n_{ch} \rangle - 0.5$, which means that $\langle R \rangle > 1$ and multiplication of particles takes place for all ω's.

For small ω's, where the virtual photon interacts with only one nucleon, the observed multiplication means that the products of the first collision, on their way out of the nucleus, interact with the other nucleons and produce the excess of particles. Thus the inequality $\langle n \rangle > \langle n_{nucl} \rangle$ for $\langle \omega \rangle = 4.3$ is an evidence for intra-nuclear cascading. What is the nature of these intermediate products only future experiments may tell. Within experimental uncertainties we do not see any difference in the relative multiplication at small and large ω's. This is somewhat surprising because, for large ω's, virtual photons interact diffractively while for small ω's we deal with incoherent interactions and some models predict a reduction of the relative multiplicities [5, 7]. Clearly, one needs better experiments.

Our measurements of $\langle R \rangle$ for $\langle \omega \rangle = 4.3$ indicate that the stuff which is being knocked out of a nucleon is able to interact immediately with nuclear matter surrounding the hit nucleon. In accordance with the commonly accepted picture a quark or a group of quarks start the process [4]. From our data we cannot say whether this quark fragments directly into hadrons (as in the case of deep inelastic production on a free nucleon) which then interact, or whether the nuclear matter surrounding the hit nucleon helps the ejected quark to fragment into hadrons. An experiment which could cast some light on these questions could be to measure relative multiplicities for fixed $\omega < 5$ for increasing $(E-E')$. If, indeed, quarks have to fragment before interacting, the relative multiplicity should approach unity as $(E-E')$ increases because of time dilation effect which would make the quark fragment outside of the target nucleus.

The hospitality and help of the staff of Fermi National Accelerator Laboratory is gratefully acknowledged. We especially thank drs R. R. Wilson and E. L. Goldwasser for their interest in our experiment. We are much indebted to A. Skuja for the excellent beam operation, S. W. Herb for invaluable help before and during the run, K. W. Chen

for the loan of a part of the apparatus and to A. Dwuraźny for his help in preparation of the experiment. Our thanks are due to Professor M. Mięsowicz for his interest in this work and we also thank him and Professors A. Białas and J. D. Bjorken for many discussions of the problems of particle production on nuclei. We thank drs L. L. Frankfurt, M. I. Strikman and V. M. Shekhter for very stimulating remarks.

REFERENCES

[1] K. Gottfried, *Coherent and Incoherent Multiple Production in Nuclei*, Proceedings of the Fifth International Conference in High Energy Physics and Nuclear Structure, Uppsala 1973; W. Busza, *Acta Phys. Pol.* **B8**, 333 (1977).

[2] L. N. Hand et al., *Description of the apparatus and tagging of events, Search for charm*, in preparation.

[3] L. D. Landau, I. Ya. Pomeranchuk, *Dokl. Akad. Nauk SSSR* **92**, 535, 735 (1953); E. L. Feinberg, *Phys. Reports* **5C**, 240 (1972); M. Mięsowicz, *Acta Phys. Pol.* **B3**, 105 (1972); K. Gottfried, *Phys. Rev. Lett.* **32** 957 (1974). F. Low; K. Gottfried, *Phys. Rev.* **D17**, 2487 (1978).

[4] J. D. Bjorken, *Hadron Final States in Deep Inelastic Processes*, Lectures at the International Summer Institute in Theoretical Physics, DESY, Hamburg, September 1975, SLAC-PUB-1756, May 1976.

[5] G. V. Davidenko, N. N. Nikolaev, *Nucl. Phys.* **B135**, 333 (1978).

[6] A. Białas, W. Czyż, *Nucl. Phys.* **B137**, 359 (1978).

[7] L. L. Frankfurt, M. I. Strikman, The Leningrad Institute of Nuclear Physics, Preprint 329, May 1977 and private communication.

[8] K. Bunnell et al., *Inelastic Muon-Neutron Scattering: Charge Hadron Multiplicities and Prong Cross-Sections*, SLAC-PUB-2061, 1977.

[9] H. Meyer et al., *Nuovo Cimento* **28**, 1399 (1963).

[10] H. Winzeler, *Nucl. Phys.* **69**, 651 (1965).

[11] E. M. Friedlander, A. Friedman, *Nuovo Cimento* **52A**, 912 (1967).

[12] J. Gierula et al., *Acta Phys. Acad. Sci. Hung.* **29**, Suppl. 3, 157 (1970); J. Babecki et al., *Acta Phys. Pol.* **B9**, 495 (1978).

[13] J. Babecki et al., *Phys. Lett.* **B47**, 268 (1973).

[14] Alma-Ata and other Labs., *Yad. Fiz.* **19**, 1094 (1974); K. G. Gulamov, private communication.

[15] J. Hebert et al., *Phys. Lett.* **B48**, 467 (1974), and Proc. of the 14-th Cosmic Ray Conf. Vol. 7, 2248, München 1975, I. Otterlund, private communication.

[16] J. W. Martin et al., paper presented at 13-th International Conference on Cosmic Rays, Denver 1973.

[17] E. M. Friedlander, A. A. Marin, *Lett. Nuovo Cimento* **9**, 346 (1974).

[18] A. Albini et al., *Nuovo Cimento* **32A**, 101 (1976).

[19] C. del Papa et al., *Phys. Rev.* **D13**, 2934 (1976).

[20] B. Gibbard et al., *Phys. Rev.* **D11**, 2367 (1975).

[21] M. Derrick et al., *Properties of the Hadronic System Resulting from* $\bar{\nu}_\mu$ *p Interactions*, ANL-HEP-PR-77-39, July 1977; J. W. Chapman et al., *Phys. Rev. Lett.* **36**, 129 (1976).

[22] L. N. Hand et al., *Intra-Nuclear Cascading in Deep Inelastic Scattering of 150 GeV Muons in Emulsion*, Raport INP-1019/PH, Kraków 1978.

[23] W. A. Loomis et al., *Hadron Production in Muon-Proton and Muon-Deuteron Collisions*, paper submitted to *Physical Review*.

[24] J. Babecki et al., *Acta Phys. Pol.* **B5**, 315 (1974).

[25] B. Furmańska et al., *Acta Phys. Pol.* **B8**, 973 (1977).

[26] A. Jurak, Raport INP-857/PH, Kraków 1973.